Egyptian Journal of Aquatic Biology & Fisheries
Zoology Department, Faculty of Science,
Ain Shams University, Cairo, Egypt.
ISSN 1110 – 6131
Vol. 25(3): 955 – 978 (2021)
www.ejabf.journals.ekb.eg

Remote Sensing for Shoreline Response to the Construction of Breakwaters and Distribution of the Invasive Species *Brachidontes pharaonis* (Bivalvia, Mytilidae), Mediterranean Sea, Egypt

Ahmed F. Salama[1]; Khaled A. ELDamhogy[2]; Sameh B. El kafrawy [3]; Ahmed N. Alabssawy[2]; Hamdy O. Ahmed[4]

1- Egyptian Environmental Affairs Agency (EEAA), Alexandria Branch, Egypt.
2- Zoology Dept., Faculty of Science, Al-Azhar University, Egypt.
3- National Authority for Remote Sensing and Space Science, Egypt.
4- National Institute of Oceanography and Fisheries, Egypt.

*Corresponding Author: S_elkafrawy@yahoo.com

ARTICLE INFO

Article History:
Received: March 22, 2021
Accepted: June 18, 2021
Online: June 30, 2021

Keywords:
Shorelines;
Artificial concrete breakwaters (ACBs);
Erosion rate;
Accretion rate.
Invasive species *Brachidontes pharaonis.*

ABSTRACT

This work aimed to address the Egyptian Shoreline response to the construction of the Artificial Concrete Breakwaters (ACBs) and distribution of the invasive species *Brachidontes pharaonis* at the Mediterranean Sea from spring 2016 to winter 2017. For the estimation of erosion and accretion, the terrestrial satellite imagery was used, including multi-dates of MSS 1973, Landsat Thematic Mapper (TM) imagery of 1984, and ETM 1990, 2001, and 2018. Two main methods were adopted; treatment and interpretation, in all the sites studied, with the exception of Rosetta. During the period before the beginning of the construction of the Artificial Concrete Breakwaters (ACBs), erosion increased but accretion decreased. However, the exact contrary occurred after construction, where erosion decreased but accretion increased. *Brachidontes pharaonis* inhabits hard substrates. Temporal average densities recorded their highest in spring and winter, but the lowest was detected in summer. On a spatial level, its maximum mean density occurred at the Baltiem Artificial Concrete Breakwaters (ACBs), while the minimum density was observed at El Dabaa Artificial Concrete Breakwaters (ACBs). The highest absolute value was listed during autumn in the Baltiem Site, while El Dabaa concrete breakwaters showed the lowest.

INTRODUCTION

Breakwaters are one of the means of protecting beaches from corrosion resulting from several factors, such as the impact of climate change and urban activities at the beach **(El-Sharnouby & Soliman, 2010)**. The response of sandy beaches to detached breakwaters has been discussed worldwide **(Ming & Chiew, 2000; Zisserman & Johnson, 2002)**. Coastal zone monitoring is an important task in terms of sustainable development and environmental protection **(Frihy *et al*., 2004)**.

The shoreline response, due to the construction of the submerged breakwater using the Digital Shoreline Analysis System (DSAS), shows shoreline accretion along most beaches of Miami, the western part of Asafra, and the eastern parts of Mandara and

Montaza. In contrast, areas of shoreline erosion were present at the eastern part of Asafra beach and the western part of Mandara beach **(Soliman *et al.*, 2014)**.

Brachidontes pharaonis (Fischer, 1870) (Bivalve, Mollusca) is just an invader. Its origin is the Indo-Pacific area, mainly in Southeastern Asia. It settled hard substrate as far as the Red Sea is considered where dense mussel mats were established **(Gilboa, 1976).** *Brachidontes pharaonis* were recorded in Tunisia waters thrice; the first time was in August 2007, the second was from a living specimen in 2011, and the third was when the species were observed to be aggregated with Mytilaster minims in a coastal area of Zarzis. *Brachidontes pharaonis* was considered rare. In 2013, Mollusca were recorded in the same area (Zarzis) at very shallow depths in the harbour and the artificial reef. During an investigation of the lagoon of Boughrara in 2016, a "Brachidontes bed" was discovered where the mollusks density was estimated at 5000 specimens/m^2 **(Hamza *et al.*, 2018)**. *Brachidontes pharaonis* is confined to a few high temperatures and salinity habitats where it has established dense beds on hard substrata. *Brachidontes pharaonis* is forecast to continue migrating to North Africa and Gibraltar **(Sarà *et al.*, 2003)**. *Brachidontes pharaonis* invasive potential is considered, taking into consideration the recent warming trend of the Mediterranean. *Brachidontes pharaonis* has been widely reported to be present in the Western Pacific Ocean, the Indian Ocean, and the Red Sea **(Morton, 1988)**. Its migration to the Mediterranean Sea through the Suez Canal and from the eastern coast of southern Africa was reported **(Barash & Danin, 1986).**

Few studies were done to assess its ecology, age structure, distribution, and biometric relationships in the Red Sea, Gulf of Suez, and Eastern Mediterranean Coast of Egypt **(Radwan, 2014; El-Sayed *et al.*, 2016)**. Lately, the erosion/accretion pattern along beaches in some regions of the Egyptian Mediterranean Coast was treated. In this study, authors estimated erosion and accretion rates during different periods observing the changes on the beaches of Baltim, Rosetta, Bir Massud, Sidi Bisher, NOIF, Six October, and EL– Dabaa, respectively.

This work aimed to measure the changes in the coastal strip using remote sensing techniques since it is the most optimal and accurate tool, particularly for measuring erosion and accretion processes. Additionally, the study aimed to record the highest abundance of the invasive molluscs' species *Brachidontes pharaonis* over the four seasons to determine its spatial and temporal distribution of the five sites between Baltiem at Kafr- Elsheikh to El-Dabaa of the governorate Matrouh, Mediterranean Sea, Egypt.

MATERIALS AND METHODS

1- Study Areas

Along the Mediterranean Sea coast of Egypt, five sites were selected: Baltim, Rosetta, NIOF, Sixth of October, and EL-Dabaa area (Fig. 1).

1. Baltim beach spreads alongside the Baltim district, northeast of Kafr El-Sheikh governorate that lies east of Alexandria between latitudes 31°35'24.48" N and longitudes 31° 09'9.41"E (Fig. 2), the area of study was 0.1 km^2.
2. Rosetta headland spreads along the Rosetta district in El-Behaira governorate, northwest of Kafr El-Sheikh governorate that lies east of Alexandria between latitudes 31°28'20" N and longitudes 30° 22'16"En (Fig. 3), the area of study was 0.21 km^2.
3. Castle of Qaitbay on the Mediterranean Coast in Alexandria is located on a stretch of land extending for about 2.43 km between latitudes 31° 12' 49" N and longitudes 29° 53' 07" E (Fig. 4).
4. El-Nakheel coastal area at the Sixth of October Village is 21 km west of Alexandria. The area extends for about 1200 m, between latitudes 31° 05' 39.5" N and longitudes 29° 43' 27.5" E (Fig. 5). The area of study was 0.015 km^2.
5. Ghazala Bay is alongside Sidi Abdelrahman coastal area, El-Alamein city, Marsa Matrouh governorate, 145 km west of Alexandria between latitudes 31° 02' 17" N and longitudes 28° 35' 32" E (Fig. 6), the area of study was 0.003 km^2.

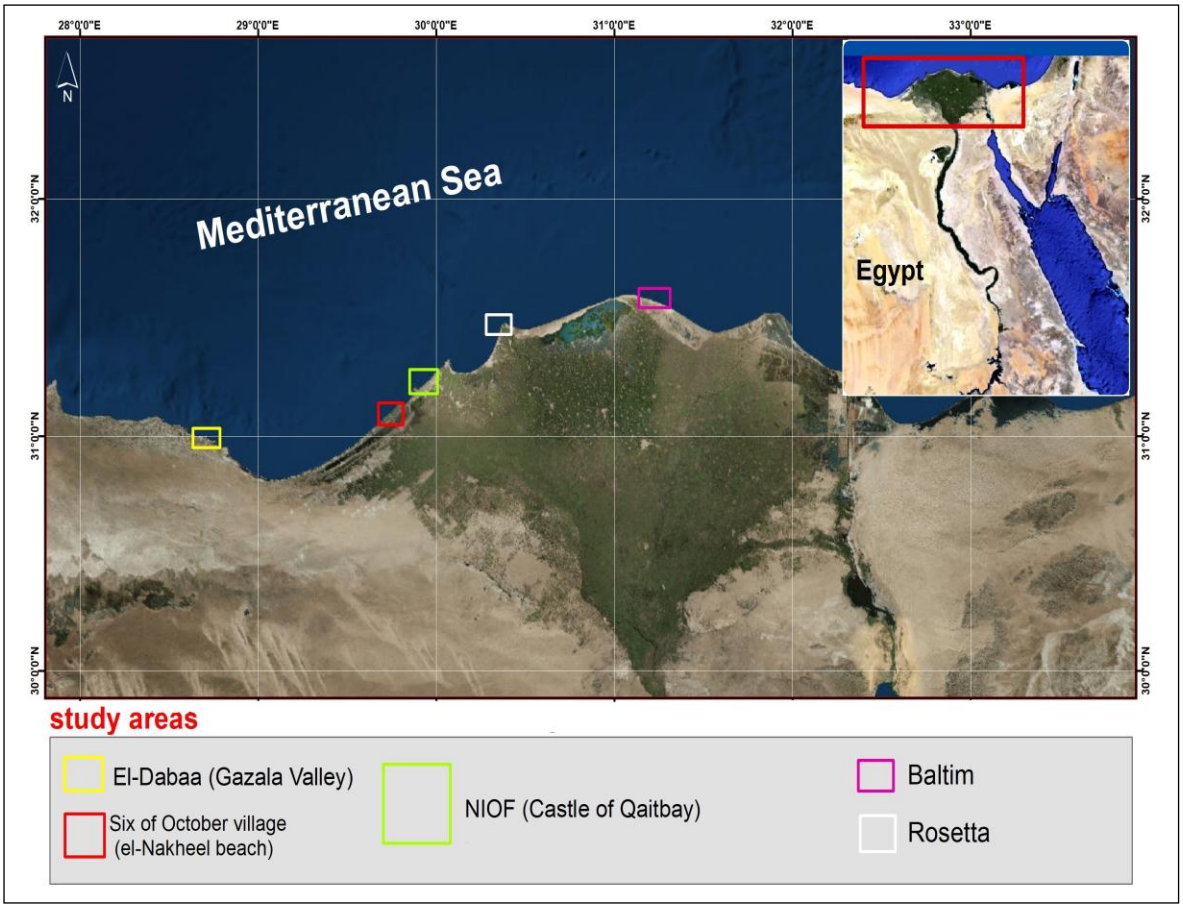

Fig. 1: Study sites at the Mediterranean Sea, Egypt, during this work.

Table 1: The Studied Sites and their Description during this Study.

Code	Latitude	Longitude	Site Name	ACBS* at Each Site
1	31°35'24.48" N	31° 09'9.41"E.	Baltim	Parallel to the beach
2	31°28'20" N	30° 22'16"E.	Rosetta	Attached to the beach
3	31° 12' 49" N	29° 53' 07" E	NIOF	Attached to the beach
4	31° 05' 39.5" N	29° 43' 27.5" E	Sixth of October	Parallel to the beach
5	31° 02' 17" N	28° 35' 32" E	El-Dabaa	Circular ACBS

***ACBS stands for Artificial Concrete Breakwaters.**

2. Satellite Images

Satellite imagery was acquired using the 60 m Landsat (TM) spatial resolution in 1973 and 1990. Two Landsat (ETM) spatial resolutions of 30 m were obtained in 1990 and 2018 (Table 2). All images were processed using the ENVI program. The evaluation of the impacts of shoreline changes on the land cover regime requires the development of a geographic database for the study area and shoreline delineation at different times. The imagery acquired represented the shores during the summer with good quality without effective clouds covering over 45 years.

Table 2: Details of Satellite Images (https://earthexplorer.usgs.gov/).

Satellite Data	Date of Acquisition	Resolution (m)
Landsat MSS	1/4/1973	60 m
Landsat MSS	5/2/1984	60 m
Landsat TM	7/12/1986	60 m
Landsat TM	5/15/1990	30 m
Landsat ETM+	14/11/2002	30 m
Landsat ETM+	1/11/2003	30 m
Landsat ETM+	1/11/2017	30 m
Landsat 8 OLI	12/14/2018	30 m

3. Geometric Correction

According to the metadata documentation, TM and ETM images used in this study are orthorectified products. They are indeed in the World Geodetic System (WGS84) datum and the Universal Transverse Mercator (UTM) projection system. The assessment of the geometric quality of the images by superimposing linear objects permitted us to observe significant discrepancies in the images. Thus, it was better to geo-reference all image sets using digital topographic maps (1: 50000) to rectify all satellite images.

4. Shoreline Extraction

Shoreline delineation through remote sensing techniques relies on the varied spectral response of water and other land surfaces at different wavelengths. The coastline can be extracted from a single-band image since the reflectance of water is nearly equal to zero in the reflective infrared bands, achievable estimating the histogram threshold for one of the infrared bands of the TM or ETM imagery. According to the histogram threshold technique, water bodies can be separated from other land covers, and the shoreline is consequently delineated from band 5 (mid-infrared) in the TM and ETM images. Digitized shorelines in the selected site beaches between 1973 and 2018 were prepared by ICZM lab in NARSS. The Digital Shoreline Analysis System (DSAS) tool was used, by creating a new transect layer in which the distance between transects was set to 100 m. DSAS deduced all required data from the input baseline, shoreline, and transect files covering all the areas of study. The approach of rate calculation depended on measuring the differences between shorelines through time.

5. Sampling

Brachidontes pharaonis was collected seasonally from the selected sites at intertidal zones from spring 2016 to winter 2017. The quadrates 25 x 25 cm were used. At each visit, three quadrates were laid at each site. The line intercept transect technique according to the method of **English *et al.* (1997)** was used to describe the general profile, calculate Artificial Concrete Breakwaters (ACBs) cover percentage, and illustrate habitat types of the selected sites. All collected samples were scraped using a putty knife and counted directly in the field.

6. Collection of Water Samples

At each visit, salinity, pH, and seawater temperature were measured using a portable pH/mv/ ^{o}C meter, Model YSI 550 A. Dissolved oxygen was measured by a DO meter/DO- 25A. Samples were kept in bottles in an icebox and analyzed in the laboratory. Transparency in water was measured using a Secchi disc.

7. Statistical Analysis

All collected data in the present study were tabulated and appropriate graphs were constructed. The data was statistically analyzed using several computer softwares such as Excel 2016. All satellite images were subjected to image processing using ENVI software for image enhancement, layer stacking, and radiometric correction.

Shoreline extracted using an Arc GIS 10.7 Toolbox was used to convert polygons to lines. Then, an editor toolbar was used to remove the edge lines. Arc GIS 10.7 was used to produce maps' layout and calculate statistical analysis.

RESULTS

1. Physiochemical Parameters

1.1 Seawater Temperatures (°C)

Its highest average values occurred during autumn (28.3°C) at site II, while its lowest was recorded during winter (22°C) at site I.

Table 3: Seasonal Variation of Temperature (°C) in ACBs.

Stations / Season	Baltim	Rosetta	NIOF	Sixth of October	El-Dabaa
Spring	25.9	26.9	25.8	26	25.1
Summer	26.9	27.76	26.91	27	26.52
Autumn	26.2	28.3	25.8	26	25.34
Winter	22	24.1	23	22.7	20.5
AV. C	25.25	26.765	25.3775	25.425	24.365

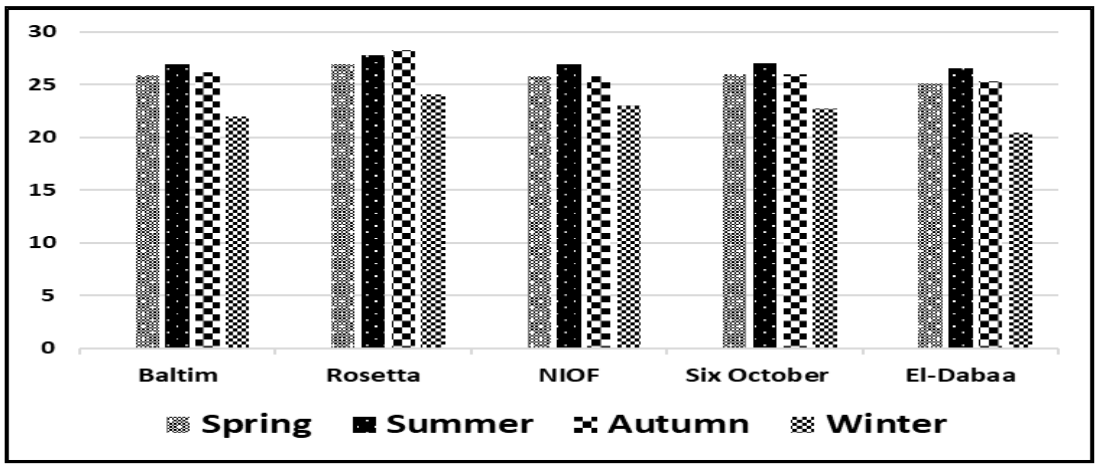

Fig. 2: Seasonal Variation of Temperature (°C) in ACBs at the Study Area.

1.2 Hydrogen Ion Concentration (pH)

The highest average pH values were present during autumn (8.29) at site II, while they were at their lowest during winter (7.86) at site V.

Table 4: Seasonal Variation of Hydrogen Ion Concentration (pH) in ACBs.

Stations / Season	Baltim	Rosetta	NIOF	Sixth of October	El-Dabaa
Spring	8	8.2	7.7	8.1	7.6
Summer	7.99	8.13	7.9	8	7.74
Autumn	7.9	8.29	7.83	8.2	7.73
Winter	7.95	8.1	7.8	7.9	7.56
AV. PH	7.96	8.18	7.8075	8.05	7.6575

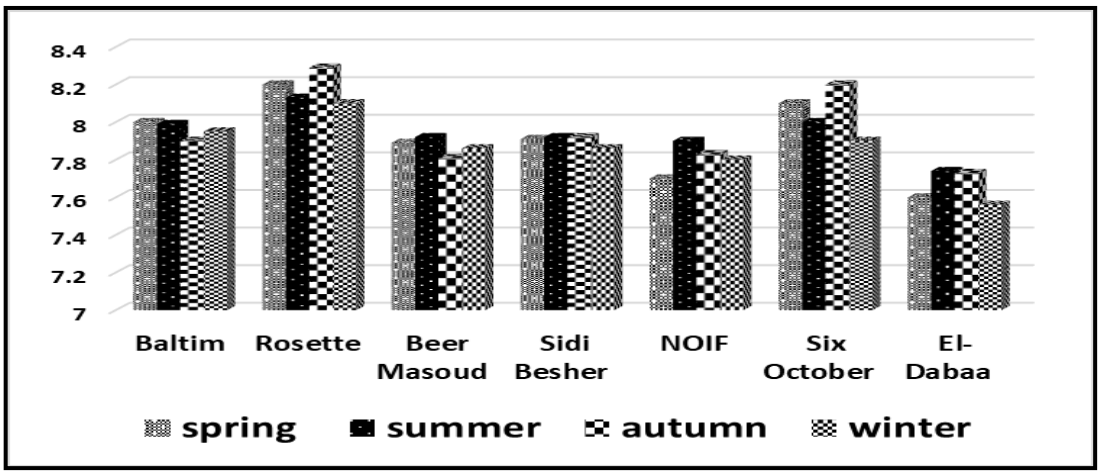

Fig. 3: Seasonal Variation of Hydrogen Ion Concentration (pH) in ACBs at the Mediterranean Sea, Egypt.

1.3 Salinity

Its highest average values occurred during spring, summer, and autumn (38‰) at site V, while its lowest was recorded during summer (32.4‰) at site II.

Table 5: Seasonal Variation of Salinity ‰ in ACBs.

Stations / Season	Baltim	Rosetta	NIOF	Sixth of October	El-Dabaa
Spring	37.2	32.4	36.8	34.2	38
Summer	36.2	35.1	37.8	36	38
Autumn	36.1	35	37.6	35.2	38
Winter	37.1	32.45	36.9	34.45	37.94
AV. Salinity	36.65	33.7375	37.275	34.9625	37.985

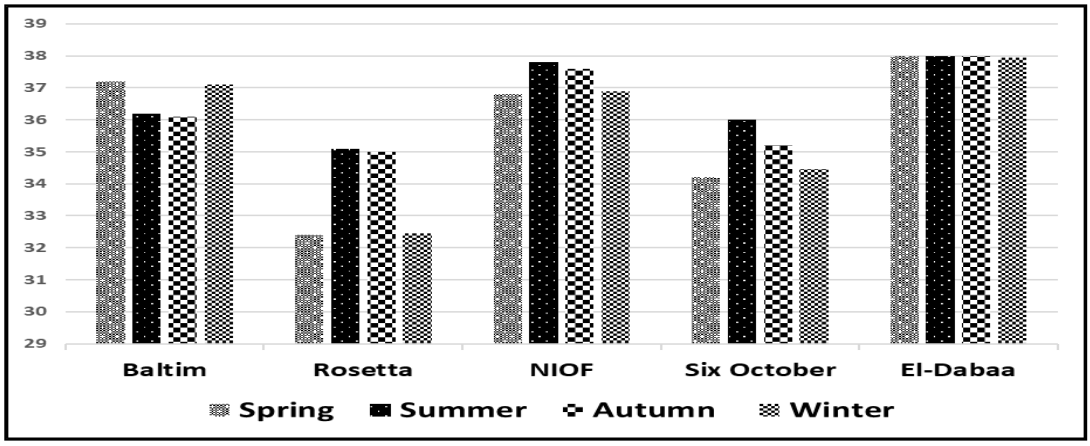

Fig. 4: Seasonal Variation of Salinity ‰ in ACBs at the Mediterranean Sea, Egypt.

1.4 Dissolved Oxygen (DO)

The highest average value was recorded during winter and autumn (6.4 mg/l) at site IV, while the lowest was recorded during summer (5.1 mg/l) at sites II and III.

Table 6: Seasonal Variation of Dissolved Oxygen DO (mg/l) in ACBs.

Stations / Season	Baltim	Rosetta	NIOF	Sixth of October	El-Dabaa
Spring	5.8	6.2	5.1	6	5.7
Summer	5.6	5.1	5.1	5.6	5.2
Autumn	5.8	6.2	5.8	6.4	5.3
Winter	5.7	6.2	5.8	6.4	5.6
AV. DO	5.725	5.925	5.45	6.1	5.45

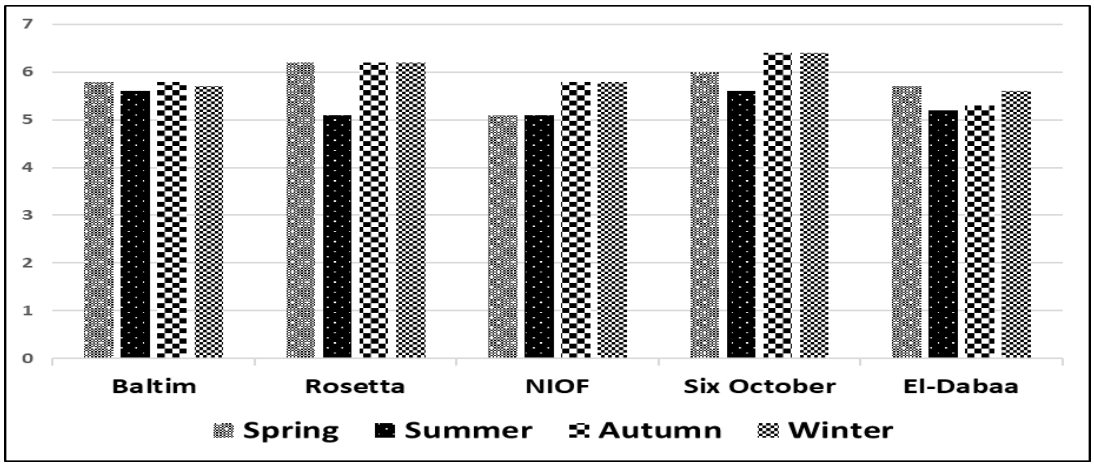

Fig. 5: Seasonal Variation of Dissolved Oxygen DO (mg/l) in ACBs.

1.5 Transparency

Its highest average value occurred during winter (355.1cm) at site V, but the lowest one was listed during summer (52.1cm) at site II.

Table 7: Seasonal Variation of Transparency (1CM) in ACBs.

Stations / Season	Baltim	Rosetta	NIOF	Sixth of October	El-Dabaa
Spring	64	56	180	190	350
Summer	55	52	183	180	340
Autumn	58	55	180	190	350
Winter	64	61	190	195	355
AV. Transparency	60.25	56	183.25	188.75	348.75

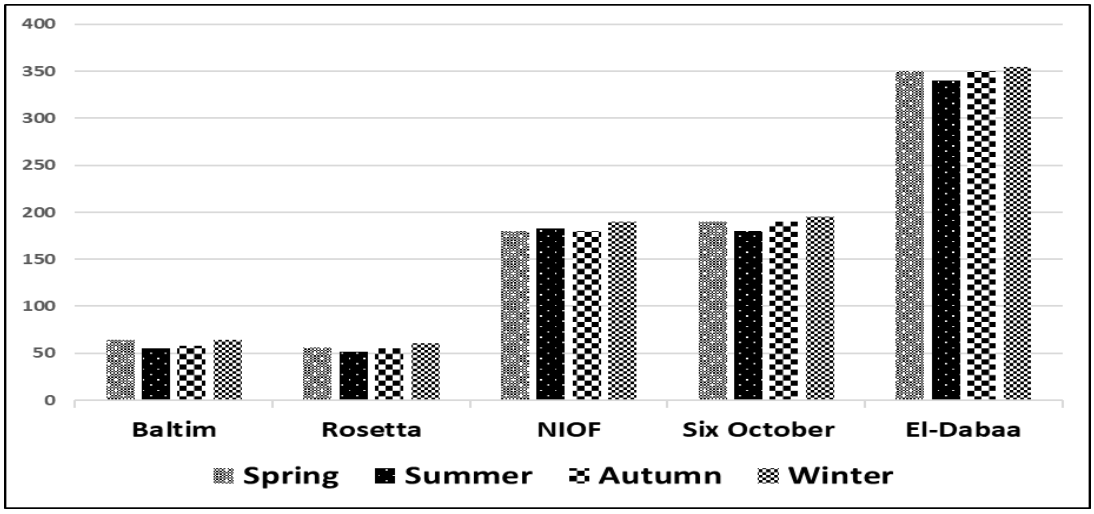

Fig. 6: Seasonal Variation of Transparency (1CM) in ACBs at the Mediterranean Sea, Egypt.

2. Shoreline changes response to breakwaters

2.1. Baltim Site

Digitized shoreline images of Baltim beach between 1973 and 2018 covered the interval before the construction of concrete breakwaters (17 years) from 1973 to 1990. Erosion increased reaching an estimate of 0.59 km^2 (erosion rate = 0.0348 km^2/year). However, accretion decreased reaching an estimated 0.17 km^2, with an approximate rate of 0.01km^2/year. After construction from 1990 to 2018 (28 years), erosion decreased and was estimated to be 0.12 km^2 (erosion rate about 0.0043 km^2/year). On the other hand, accretion increased reaching an estimate of 1.19km^2 (accretion rate of 0.0425 km^2/year). Simultaneously, the accretion pattern had eight groins. The shoreline from 1973 to 2018 maintained the pattern of erosion and accretion since 1973. An overlay of GIS layers with IKONOS images taken in 2018 was acquired, where shoreline changed in retreating and forward movement rates (morph dynamics).

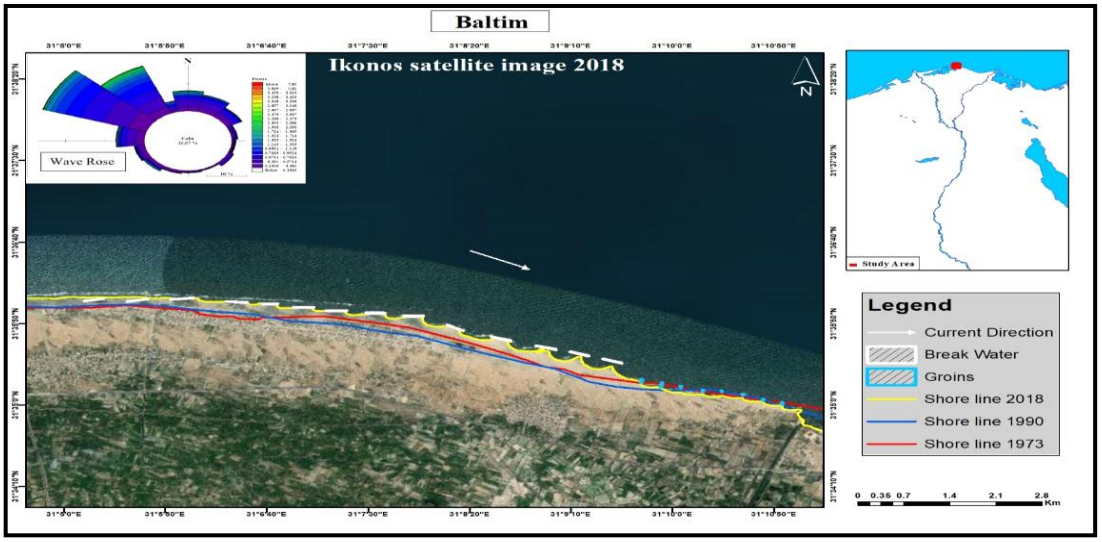

Fig. 7: Shoreline Changes in Baltim Beach from 1973 to 2018.

2.2. Rosetta Site

The Rosetta promontory is one of the most important areas in Egypt for monitoring beach erosion. During this period, erosion cut the Rosetta promontory. Digitized shoreline images covering the Rosetta beach between 1973 and 2018 covered the period before the beginning of construction from 1973 to 1990 (17 years). Erosion increased reaching an estimate of 5.7 km^2 (erosion rate was 0.3353 km^2/year), but accretion decreased to an estimate of 3.51 km^2 (accretion rate about 0.2065 km^2/year).

After the construction from 1990 to 2018 (28 years), erosion increased to an estimate of 9.45 km^2 (erosion rate being 0.3375 km^2/year). However, accretion increased to an estimate of 0.07 km^2 (accretion rate was 0.0025 km^2/year). Simultaneously, an accretion pattern with 14 groins existed. The map contained an overlay of GIS layers (shorelines from 1973 to 2018) with IKONOS images taken in 2018.

The coastline along the Rosetta Promontory is the most fragile segment of the Nile Delta Coast. The highest erosion occurred in front of the promontory located at the western side, while sedimentation happened on the eastern side. A reverse of erosion occurred after the construction of the Rosetta Seawall, where a new erosion zone was formed on the eastern side of the promontory.

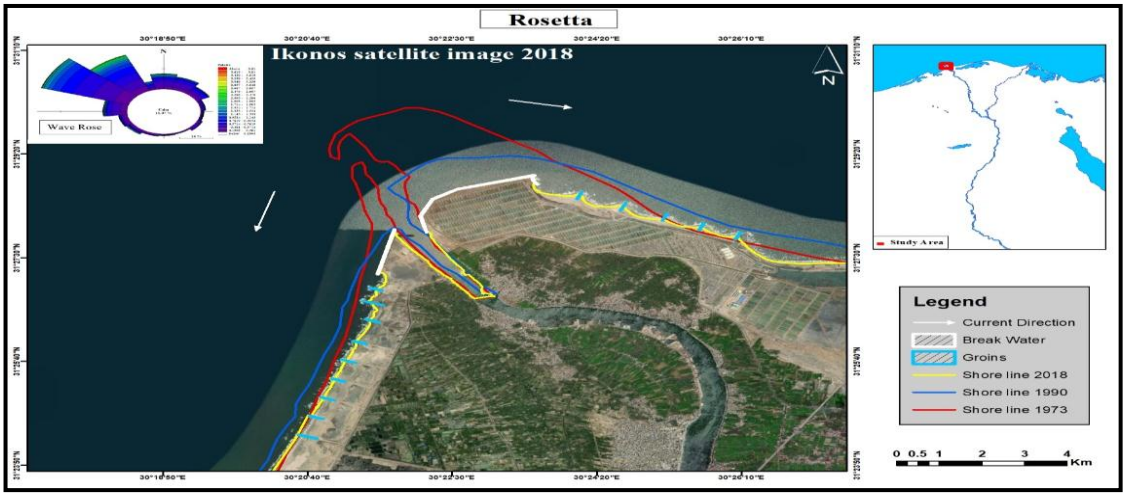

Fig. 8: The Changes of the Rosetta Shoreline from 1973 to 2018.

2.3. NIOF (Castle of Qaitbay)

NIOF detached Artificial Concrete Breakwaters (ACBs) is located around the Castle of Qaitbay, at the left side of it as a groin curve shape. Digitized shoreline images of Qaitbay Castle Beach between 1984 and 2018 covered the period before construction from 1984 to 2000 (16 years).

During that period, erosion increased and was estimated at 0.016 km^2 (erosion rate about 0.001 km^2/year), while accretion was estimated to be 0.024 km^2, (accretion rate being 0.0015 km^2/year). After construction from 2000 to 2018 (18 years), erosion decreased to zero, but accretion increased in the attached breakwaters and was estimated by 0.03 km^2 (accretion rate about 0.0017 km^2/year).

On the other hand, an accretion pattern existed with a single groin. The map contains an overlay of GIS layers shorelines between 2001 and 2018 with IKONOS images taken in 2018. In 2000, images showing the shoreline surrounding the castle without protection constructions were considered. On the contrary, in 2018, images show changes in shoreline with widening and concrete blocks and land head at the left side of the castle.

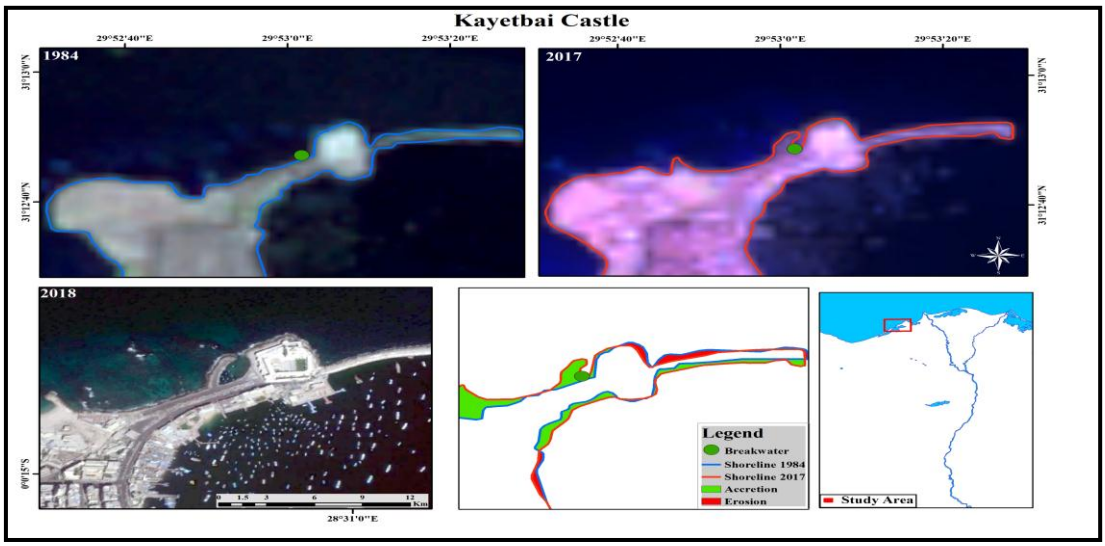

Fig. 9: The Shoreline Changes at NIOF (Qaitbay) Beach from 1984 to 2018.

2.4. Sixth of October (El-Nakheel Beach)

El-Nakheel detached breakwaters are located 20 km west of Alexandria City. It is bounded by the Nobarya Drain at the westward reach and the Sixth of October Village at the eastward reach with a total length of about 2.0 km. There is a rocky ridge extending parallelly to the shoreline. Seven detached Artificial Concrete Breakwaters (ACBs) have been constructed to provide a safe and secure environment in the area. Digitized shoreline images of El-Nakheel Beach between 1984 and 2018 listed the period before construction from 1984 to 2002 (18 years). Erosion increased and was estimated to be 0.022 km^2, and erosion rate was about0.0012 km^2/year.

On the other hand, accretion was estimated to be 0.011km^2, and the accretion rate was about0.0006 km^2/year. After construction from 2002 to 2018 (16 years), erosion declined and was estimated to be 0.006 km^2 (erosion rate was 0.0004 km^2/year), while accretion increased and was estimated to be 0.055 km^2 (accretion rate was 0.0034 km^2/year).

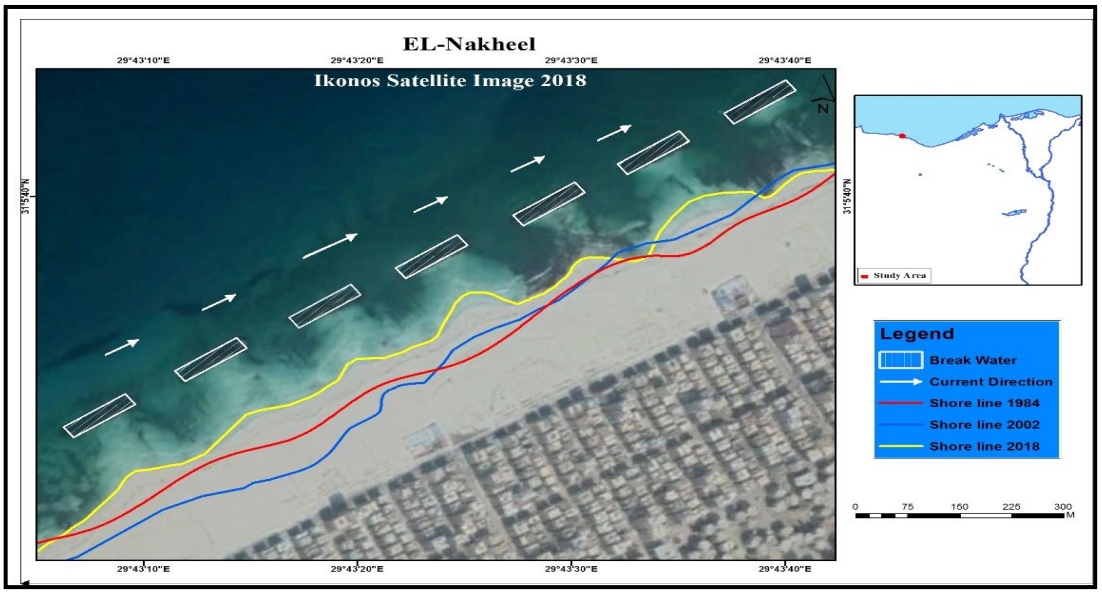

Fig. 10: The Shoreline Changes at El-Nakheel Beach from 1984 to 2018.

2.5. El-Dabaa

Egypt digitized shoreline images covering El-Dabaa beach between 1986 and 2018 detected the interval before construction from 1986 to 2003 (17 years). Erosion increased and was estimated to be 0.35 km^2 (erosion rate being0.0175 km^2/year).

There was no accretion in the region regarding the sand beach. After construction from 2003 to 2018 (15 years), erosion decreased and was estimated to be 0 km^2 and transformed to the eastern side of the previous erosion action. However, in the study area, the shore transformed from sandy to rocky, and the breakwaters were formed, taking a curved-shape formation parallel to the beach. Also, the rate of accretion increased and was estimated to be 0.037km^2 (accretion rate was 0.0025 km^2/year).

The map contains an overlay of GIS layers (shorelines from 1986 to 2018) with IKONOS images taken in 2018, where shoreline changed in retreating and forward movement rates (morph dynamics) at a high-speed erosion rate at the upper right portion of the beach boundary and a high-speed accretion rate at the inside curved-shape Artificial Concrete Breakwaters (ACBs), and at the left curved-shape pattern of erosion and accretion since 1986.

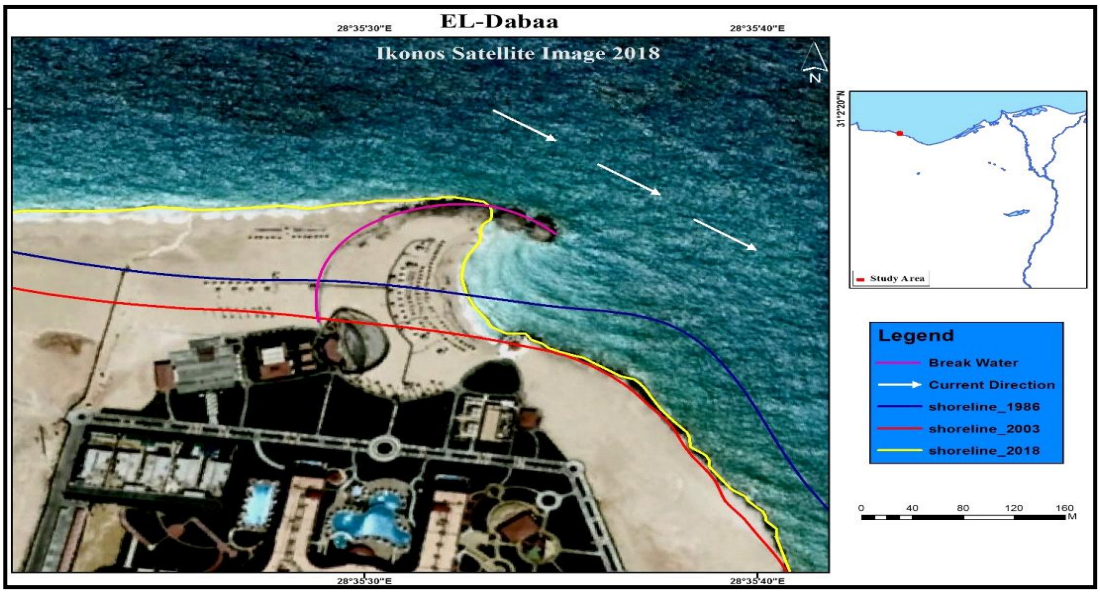

Fig. 11: The Shoreline Changes at El-Dabaa from 1986 to 2018.

Table 8: Erosion and Accretion Rate for Sites and their Description of this Study.

Region	Construction Date	Start Construction	Period/ Year	Erosion /km^2	E. Rate km^2 /Year	Accretion /km^2	A. Rate km^2 /Year
Baltim	1990	Before	17	0.59	0.034	0.17	0.01
		After	28	0.12	0.004	1.19	0.042
Rosetta	1990	Before	17	5.7	0.33	3.51	0.206
		After	28	9.45	0.33	0.07	0.0025
NIOF	2000	Before	16	0.016	0.001	0.024	0.0015
		After	18	0	0	0.03	0.001
Six October	2002	Before	18	0.022	0.0012	0.011	0.0006
		After	16	0.006	0.000	0.055	0.003
El-Dabaa	2003	Before	17	.35	0.0175	0	0
		After	15	0	0	0.037	0.0024

Brachidontes pharaonis (Fischer, 1870)

Synonymous with

- *Brachidontes semistriatus*, Krauss, 1848
- *Brachidontes variabilis*, Krauss, 1848
- *Mytilus exustus*, Linnaeus, 1827
- *Mytilus pharaonis*, Fischer, 1870
- *Mytilus variabilis*, Krauss, 1848

International Common Names

- English: variable mussel

Its maximum average density (15656ind/m^2) occurred at Baltim Artificial Concrete Breakwaters (ACBs), but the minimum one was observed at El Dabaa artificial concrete breakwaters (ACBs) with average of 22ind/m^2. This is due to the presence of sediments

that accumulated on the breakwaters at the El Dabaa site. The highest absolute value (17172ind/m^2) was collected during autumn in the Baltim site. Table (9) and Fig. (12, 13 & 14) show its annual average density being 8779ind/m^2. The highest average density occurred during spring was 9917ind/m^2 (28.3 and 28.1%). However, the lowest value occurred in summer was 6539ind/m^2 (18.6%). This is attributed to the rise of temperature during summer. In autumn, however, an average density of 8766ind/m^2 was recorded.

Table 9: Seasonal Variations of *Brachidontes pharaonis* Density (ind/m^2)

Season Sites	Spring	Summer	Autumn	Winter	Average ± SD
Baltim	17063	13035	17172	15355	15656 ± 1936
Rosette	12428	9691	11529	10916	11141 ± 1149
NOIF	8025	4738	2908	8220	5973 ± 2593
Sixth of October	12073	5228	12212	14907	11105 ± 4129
El-Dabaa	0	2	11	75	22 ± 36
Average ± SD	9917 ± 6402	6539 ± 4996	8766 ± 7091	9895 ± 6229	8779

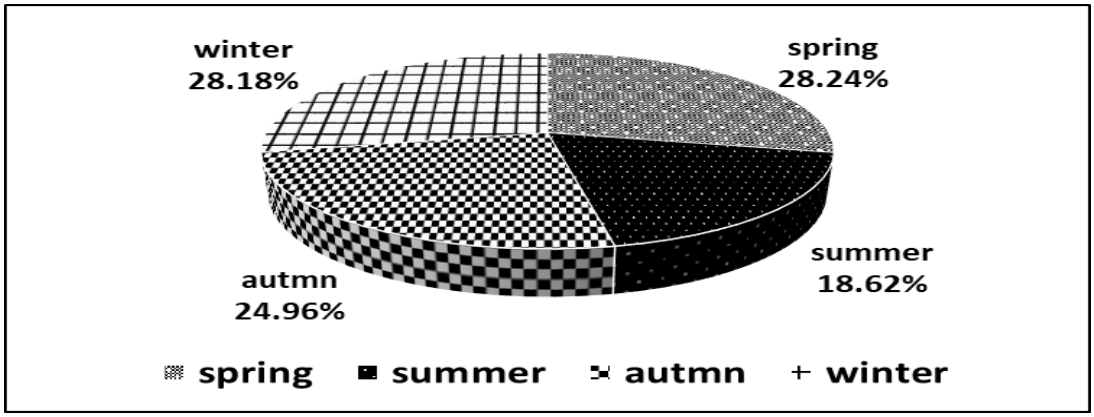

Fig. 12. Seasonal percentage of average annual of *Brachidontes pharaonis*

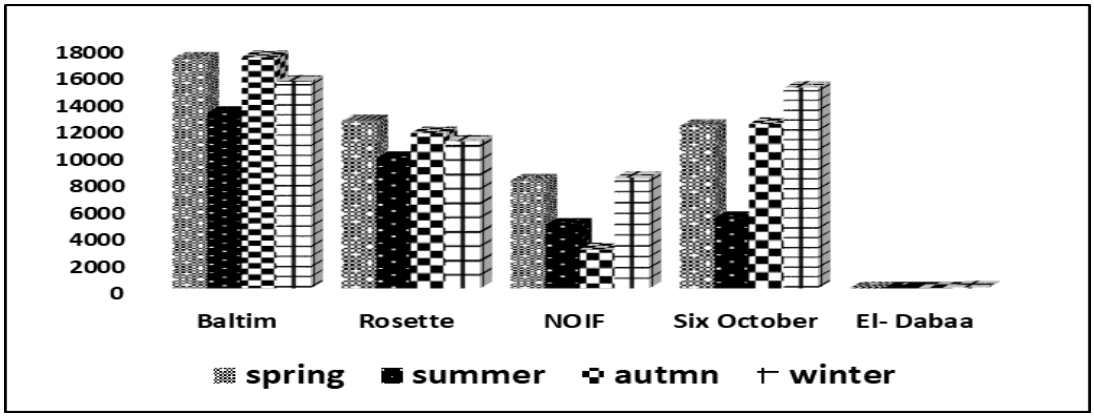

Fig. 13: Seasonal Variations of *Brachidontes pharaonis* during this Study.

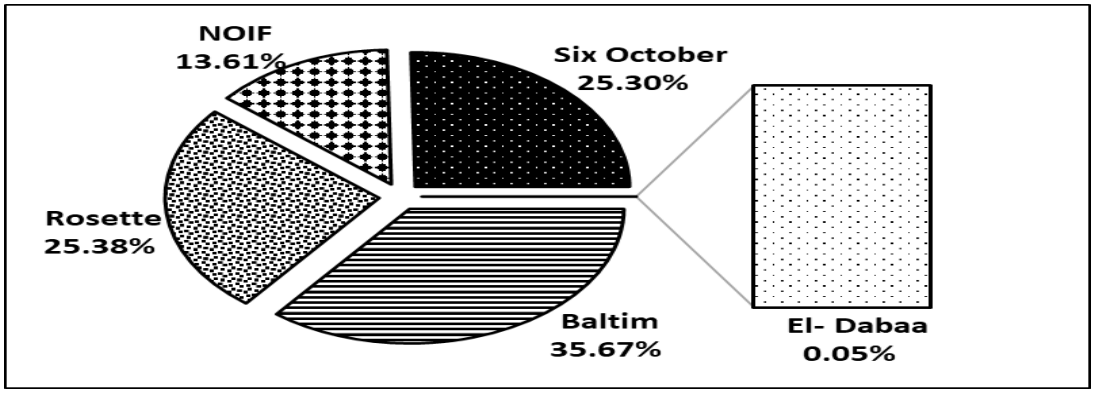

Fig. 14: Sites; Percentage of Average Annual of *Brachidontes pharaonis* during this Study.

In the list of species found in association with *Brachidontes pharaonis* (Mytilidae: Bivalvia: Mollusca), it is shown that there is a high percentage value abundance (214475ind/m^2) at 74.8% of all total species (table 10), while Mollusca was composed of two classes, Gastropoda and Bivalvia; four families, Patellidae, Trochidae, Fissurellidae, and Mytilidae; with six species, *Brachidontes pharaonis* with 98.30%, *Gibbula–umbilicalis* with 0.79%, *Fissurella nubecula* with 0.36%, *Patella rustica* with 0.28%, *Patella-careulea* with 0.25%, and *Phorcus-turbinatus* with 0.03%.

Table 10: The Percentage of the Total Species during the Study Period.

Species	No.	%	Average
Elasmopus pocillimanus	15664	5.5	2238
Photis longicaudata	19344	6.7	2763
Paradella Dianae	4194	1.5	599
Gibbula -umbilicalis	1726	0.6	247
Phorcus-turbinatus	58	0.01	8
Patella-careulea	535	0.2	76
Patella rustica	604	0.2	86
Fissurella nubecula	776	0.3	111
Brachidontes pharaonis	214475	74.8	30639
Balanus amphitrite	10816	3.8	1545
Eriphia verrucosa	48	0.01	7
Pachygrabsus marmoratus	192	0.1	27
Perinereis cultrifera	6708	2.3	958
Alitta-succinea	171	0.1	24
Serpula columbiana .	156	0.1	22
Ficopmatus enigmaticus	11122	3.9	1589

DISCUSSION

The results of physicochemical parameters of seawater in the selected study areas exhibited remarkable seasonal fluctuations in surface water temperature, salinity, dissolved oxygen, and transparency. In the current work, surface water temperature showed that the highest average values occurred during autumn (28.3^{o}C) at Rosetta, while the lowest was measured during winter (22^{o}C) at Baltim. These recorded values resemble those measured by **El-Gohary *et al*. (2011)** at Abu Kir Bay (16.06–26.36ºC) during winter and summer seasons, as well as those recorded by **Warburg *et al.* (2012)** at the eastern Mediterranean (16–28ºC). Temperature is the most important physical factor affecting biological and chemical processes in the marine environment.

Moreover, the annual average of water temperature in the Lake Edku was reported to be 22.81^{o} C **(Khalil *et al.*, 2008)**, whereas the present study refers to the annual average of water temperature with a value of 26.77°C in Rosetta.

Water temperature crucially affects animal activity, reproduction, migration, feeding, and all other aspects of life in aquatic environments. Salinity is another important factor affecting marine organisms. The distribution of the intertidal and shallow subtidal organisms is governed by the effect of salinity gradient and a range of animal tolerance. In the present work, the highest average values of salinity took place during spring, summer, and autumn (38‰) at El-Dabaa, while the lowest average values occurred during summer (32.4‰) at Rosetta. However, a slight seasonal fluctuation in salinity was recorded during different seasons of the year. High salinities were recorded throughout the summer, which was higher than those recorded at El Mex Bay (20.73–28.87 ‰) affected by drainage water. The range reported from 33.96 to 37.87‰ by **El-Gohary *et al*. (2011**) ranging from 35.1–38.66 ‰ was within 28–36‰. However, the obtained values are lower than those recorded at the southeastern Mediterranean offshore that varied within 38.66–39.79‰. High variation of surface water salinity is attributed to several factors, including drainage of freshwater and brackish waters, sewage, irrigation and industrial discharge, in addition to climatic conditions such as dryness, rains, urbanization, and increasing human activities and pollution **(El-Komi, 2012)**.

Khalil *et al.* (2008) reported that water salinity decreases in the seasons of spring, summer, and autumn, while it increases during winter. This may be attributed to the reduction of water flow from the lake to the Mediterranean Sea during the winter season. In addition, the previous authors explained the aforementioned phenomenon as an outcome of the reduction of the water flow of the flood from the River Nile to the Mediterranean Sea.

The present results showed that higher average pH values happened during autumn (8.29) at Rosetta, while the lowest took place during winter (7.5) at El-Dabaa site. On the other hand, seawater was slightly alkaline (pH ranges from 8.03–8.53) **(Abdel-Halim *et***

***al.*, 2016)**. **Hussein *et al.* (2013)** explained that the average values fluctuate between 7.66 and 8.18; showing a tendency neutral pH values. The minimum value was 7.56 in the winter, while the maximum was 8.29 in autumn. Temporal and spatial variations and statistical correlations among the analyzed variables were examined. Furthermore, **Abdel-Halim *et al*. (2016)** demonstrated a wide range of water temperature (17.14–26.31°C), narrow fluctuations in salinity (37.51–39.71), well-oxygenated seawaters (4.16–8.00 mg O2/l), and low amounts of oxidizable organic matter (1.92 mg O2/l).

The present findings revealed that, the highest average of DO values was recorded during winter and autumn (6.4 mg/l) at the Six October site, while the lowest one was noticed (5.1 mg/l) during summer at Rosetta and in spring and summer at NIOF. However, the decreasing DO values during summer may be attributed to the increasing decomposition of organic matter and decreasing solubility during summer. While, the increasing Do during spring can be associated with the increasing phytoplankton and the decreasing seawater temperature leading to increasing atmospheric oxygen solubility, which agrees with the explanation of **Hamed (2003)**.

In addition, the highest transparency average value occurred during winter (355 cm) at El-Dabaa, while the lowest value was recorded during the summer (52 cm) at Rosetta. Other works that studied the investigated area with Secchi disc readings varied from 0.52 to 3.55 m for almost the whole year. High transparency during the whole year at El-Dabaa indicates that this site has quite low human activity and is not affected by any kind of pollution. Spatial heterogeneity is particularly evident among marine benthic assemblages associated with shallow-water habitats since they commonly experience fluctuation of key environmental factors such as temperature, salinity, wave action, etc **(Benedetti-Cecchi *et al.*, 2000; Therriault & Kolasa, 2000; Sousa, 2001)**. Remarkably, pollution creates major differences in the benthic community structure **(Moran & Grant, 1991)**. **El-Naggar** discussed some parameters such as water temperature (13.50–29.00°C), slightly narrow fluctuations in salinity (37.20–38.78), well-oxygenated seawaters (6.40–8.96 mg O2/l), relatively low amounts of oxidizable organic matter (0.10–1.60 mg O2/l), and the slight alkalinity of seawater (pH range 8.04–8.63): overall, water quality from El-Dabaa to El-Saloum was good **(El-Naggar *et al.*, 2019)**.

By using Remote Sensing and GIS Approach for assessing and monitoring some chemical water quality parameters, **Khalil** listed that pH values ranged from 7.4 to 8.6, salinity was between 48.46 ‰ to 51.86 ‰ and DO varied from 4.5 mg/l to 6.7 mg/l **(Khalil *et al.*, 2016)**.

Regarding the present studied sites, except for Rosetta, during the period before the construction of Artificial Concrete Breakwaters (ACBs), erosion increased while accretion decreased. On the other hand, after construction, erosion decreased but accretion increased. From the analysis of a satellite imagery in Baltim (ACBs) constructed 1990 before 17years; the erosion was

0.59 km^2 with a rate of 0.034 km^2 /year. After 28 years of construction, the erosion was 0.12 km^2 with rate 0.004 km^2 /year. **Frihy** discussed that the erosion rate at Baltim before replacing (ACBs) was 0.005 km^2 /year and after construction it has been substantially increased in the downdrift sides of those protective systems; being 0.02 km^2 /year **(Frihy *et al.*, 2004)**. While **El-Asmar** reported the rates of shoreline change from 35 m/y to 40 m/y **(El-Asmar *et al.*, 2014)**. This result deduced that at Rosetta the construction of ACBs at 1990 (before 17 years), the accretion was 3.51 km^2 with a rate of 0.206 km^2 /year and after 28 years of construction, the accretion was 0.07 km^2 with rate 0.0025 km^2 /year. Additionally, **Frihy** mentioned that the accretion rate was about 13 m/year **(Frihy & Komar, 1993)**. While the current result referred to the erosion before construction to be 5.7 km^2 with a rate of 0.33 km^2 /year, while after the construction it was 9.45 km^2 with the rate of 0.33 km^2 /year. **El Sayed** explained that the high dam causes an erosion rate of 147 m\year in the west side and 80 m\year in the east side, and added that the new erosion area will be about 2.0 km with 30m rate **(El Sayed, 2017).**

Additionally, **Frihy *et al.* (1994)** reported that the highest rate of erosion that occurred on the Rosetta promontory tip was -70,8 m/year while accretion was 38·2 m/year from 1972 to 1992. During the period from 1990 to 2002, **Frihy *et al. (*2004)** stated that the highest rate of accretion along Baltiem beach was 35 m/year. It was noticed behind the first-built that a breakwater was following its construction. While erosion appeared far behind the rest of these breakwaters, about -20 m/year, the temporary groins built as an access way to construct those breakwaters might have accelerated the downdraft erosion in this region. The reconstruction beach erosion at Baltim (-5 m/year) has been replaced by the formation of a sand tombolo (35 m/year) and salient (9 m/year). The main type of those structures is the rubble mound breakwater. The aforementioned structures include groins perpendicular to the shoreline; breakwaters (whether detached or connected to the shore) emerged, or submerged, seawalls parallel to the coastline, and revetments to protect slopes. Nevertheless, those hard structures have side effects, causing erosion and accretion in the down- and updraft, respectively. They divert the problem to adjacent areas as they totally or immensely stop the sediment motion. This side effect takes place nearly in all the coastal protection works along with the Nile Delta **(El Sayed, 2017)**.

Notably, the coastal protection works within Rosetta Promontory succeeded to decrease the maximum shoreline retreat from 124 m/year to 37 m/year during the period from 1984 to 2014 **(Masria *et al.*, 2015)**. Moreover, the shoreline of Rosetta Promontory retreated at an average rate of 60 m/year between 1970 and 2010 **(Deabes, 2017)**.

In the case of Baltim breakwaters, land base groins were constructed to execute the detached breakwater. This led to sedimentation around the groins affecting the function of the detached breakwaters **(Iskander, 2017)**.

In NIOF in this study, it was found that before construction the erosion rate was 0.001 km^2 /year) and changed after construction to record 0.0 km^2 /year. For Accretion before construction, it was 0.001km^2 /year and become after construction 0.0 km^2 /year; accretion pattern existing with (1) groins. The 2018 date image indicates changes in the shoreline with widening and concrete blocks and groin on the left side of the castle. The coastal structure protects the area around the coasts of Qaitbay using a different type of structure (hart structure). It is worthy to mention that, shore protection authority (SPA) constructed a lot of coastal protection to protect the shoreline during the period 1984–2018 for protection and development and erasing the area because of the oldest cities and this old area region main resorting on Egyptian found high urban areas **(Frihy *et al.*, 1996).**

In this study, the ACBs construction at Six October was in 2002; before 18 years the accretion rate was 0.011 km^2 with a rate of 0.0006 km^2 /year. After 16 years of construction, the accretion was 0.055 km^2 with a rate of 0.003 km^2 /year. **Iskander (2017)** mentioned that at the beginning of the breakwater, a noticeable accretion was observed with rates ranging from 0.5 to 3 m/year, and the area behind the breakwater (shadow zone) has been experiencing a significant accretion 3–10 m/year.

Moreover, **Iskander *et al.* (2007)** concluded that Six October beach was affected by accretion that ranged from 5 to 18 meters/year after the construction of concrete breakwaters. However, breakwaters, owing to their detaching, may create weak circulation causing water stagnation affecting the water quality badly, which happened in the Six October Resort on the Northwest Coast.

The present result referred to the construction of ACBs at El-Dabaa in 2003 before 17 years stating that, the erosion was 0.35 km^2 with a rate of 0.018 km^2 /year, while after 15 years of construction the erosion was 0.0 km^2 with a rate of 0.0 km^2 /year. Noticeably, El-Dabaa beach was sandy and suffered from regular parallel high erosions curve shaped estimated by 0.35 km^2 without any accretion **(Iskander, 2017).**

Regarding the El-Dabaa site at the period before the construction of Artificial Concrete Breakwaters (ACBs), erosion increased (erosion rate being0.0175 km^2/year) without accretion. After construction, the erosion became zero while the accretion rate was about 0, 0025 km^2/year. During this work, after the construction of concrete breakwaters, most Artificial Concrete Breakwaters (ACBs) surfaces were covered by sediments. The construction of concrete breakwaters as hard substrates provided suitable habitats for the Lessepsian species *Brachidontes pharaonis*. This species is Indo-Pacific in origin and widely spread throughout the Red Sea **(Oliver, 1992)**. It migrated into the Mediterranean Sea through the Suez Canal. The presence of this molluscan species at the studied sites may be attributed to its high tolerance to harsh environmental conditions. It was abundant in the Eastern Mediterranean Basin and it reached Sicily and other southern coasts of Europe and Turkey as well **(Sara *et al.*, 2003, 2008)**. Its first record at the Mediterranean was reported by Fuchs (1876) for Egypt **(Zenetos *et al.*, 2005; Crocetta *et***

***al.*, 2009)** and it has spread throughout the Mediterranean **(Zenetos *et al.*, 2005; Galil, 2006; Crocetta *et al.*, 2009)**. It migrated by either larval dispersal, transport on the hulls of ships, or both **(Mifsud & Cilia, 2009).** These species inhabit hard substrates **(Safriel *et al.*, 1980).**

Its annual average density during the present work was 8779ind/m^2, higher than that recorded in Tunisia by **Hamza *et al.* (2018)** who detected 5000ind/m^2 as an annual average density. This is lower than that reported in the western Mediterranean by **Sara *et al.* (2008),** being 9375ind/m^2. The present work recorded its maximum average density during spring and winter, while **Sara *et al.* (2008)** noticed this value in autumn. This may be due to its migration habits. The present work calculated that *Brachidontes pharaonis* amounted to 9895ind/m^2 in winter while **Hamdy and Dorgham (2018)** counted 1630ind/m^2 in the Eastern Harbor of Alexandria during the same season of 2014. This is due to the difference in collection methods and habitats.

Khalil *et al.* (2013) mentioned that Mollusca was the most dominant group in the lake, forming about 58.9% of the total benthos, seasonal variation of macrobenthic, and the highest population density was recorded during spring with an average of 6617 Org/m2 , but in the present study the Mollusca was 74.8 %

CONCLUSION

The construction of artificial concrete breakwaters decreased erosion but increased accretion. Breakwaters, owing to their detaching, caused erosion and accretion in the down- and updrafts. The construction of concrete breakwaters in the form of hard substrate provided suitable habitat for the Lessepsian species *Brachidontes pharaonis*. Those species occurred at all sites and seasons studied. Its annual average density during the present work was about 8779 ind/m^2.

REFERENCES

Abdel-Halim, A. M. and Aly-Eldeen, M. A. (2016). Characteristics of Mediterranean Seawater in the vicinity of Sidikerir Region, west of Alexandria, Egypt. Egypt. J. Aquat. Res, 42(2): 133-140. https://bit.ly/3k4mmB2

Barash, A. and Danin, Z. (1986). Further additions to the knowledge of Indo-Pacific Mollusca in the Mediterranean Sea. Spixiana, 9(2): 117-141.

Benedetti-Cecchi, L.; Bulleri, F. and Cinelli, F. (2000). The interplay of physical and biological factors in maintaining mid-shore and low-shore assemblages on rocky coasts in the north-west Mediterranean. Oecol., 123(3): 406-417. https://bit.ly/3yHnxKT

Crocetta, F.; Renda, W. and Vazzana, A. (2009). Alien Mollusca along the Calabrian shores of the Messina Strait area and a review of their distribution in the Italian seas. Bollettino malacologico, 45(1): 15-30. https://bit.ly/3AGS7Ge

Deabes, E. A. (2017). Applying ArcGIS to Estimate the Rates of Shoreline and Back-Shore Area Changes along the Nile Delta Coast, Egypt. Intern. J. Geos., 8(3): 332-348. https://bit.ly/3ANv7FF

Dorgham, M. M.; Hamdy, R.; El Rashidy, H. H.; Atta, M. M. and Musco, L. (2014). Distribution patterns of shallow water polychaetes (Annelida) along the Alexandria coast, Egypt (eastern Mediterranean). Medi. Mar. Sci., 15(3): 635-649. https://bit.ly/3hUeTC2

El-Asmar, H. M.; El-Kafrawy, S. B. and Taha, M. M. (2014). Monitoring coastal changes along Damietta Promontory and the barrier beach toward Port Said east of the Nile Delta, Egypt. J. of Coas. Res., 30(5): 993-1005. https://bit.ly/36prvvJ

El-Gohary, S. E.; Zaki, H. R. and Elnaggar, M. F. (2011). Physicochemical and eutrophication parameters of coastal water and geochemical characteristics of bottom sediments east of Rosetta area, Mediterranean Sea, Egypt. World App. Sci. J., 14(1): 23-36. https://bit.ly/3k3vwh7

El-Komi, M. (2012). Distribution of benthic polychaetes populations affected by human activities in the west coast of Alexandria, Mediterranean Sea, Egypt. Egypt. J. Aquat Biol. & Fish., 16(1): 1-19. https://bit.ly/3xJmr0U

El-Nagger, N.; Mohamed, A.L.; Abdel-Halim, A. and Emara, E.H. (2019). Environmental Characteristics of the Egyptian Mediterranean Coast. Egypt. J. Aquat Biol. & Fish., 23(2): 475-490. https://bit.ly/2UBr6Uj

El Sayed, W. R. (2017). Nile Dealt Shoreline protection between past and future, Twentieth International Water Technology Conference, IWTC20, Hurghada, 501-511. https://bit.ly/3AChmtr

El-Sharnouby, B. and Soliman, A. (2010). Shoreline response for long, wide, and deep submerged breakwater of Alexandria city, Egypt. In Proc. 26th International Conference for Seaports and Maritime Transport "Integration for a Better Future.

Frihy, O. E. and Komar, P. D. (1993). Long-term shoreline changes and the concentration of heavy minerals in beach sands of the Nile Delta, Egypt. Marine Geology, 115(3-4): 253-261. https://bit.ly/3hYhHOm

Frihy, O. E.; Nasr, S. M.; El Hattab, M. M. and El Raey, M. (1994). Remote sensing of beach erosion along the Rosetta promontory, northwestern Nile delta, Egypt. Inter. J. Rem. Sens., 15(8): 1649-1660. https://bit.ly/3k05yeF

Frihy, O.E.; Dewidar, K.M. and El Raey, M.M. (1996). Evaluation of coastal problems at Alexandria, Egypt. Ocean & coas. manag., 30(2-3): 281-295. https://bit.ly/2TW4DkH

Frihy, O. E.; El Banna, M. M. and El Kolfat, A. I. (2004). Environmental impacts of Baltim and Ras El Bar shore-parallel breakwater systems on the Nile delta littoral zone, Egypt. Envir. Geol., 45(3): 381-390. https://bit.ly/3yWRMOf

Galil, B.S. (2006). The marine caravan–the Suez Canal and the Erythrean invasion. In Bridging divides (pp. 207-300). Springer, Dordrecht.

Gilboa, A. (1976). Experiments in mytilids recolonization. Doctoral dissertation, MS Dissertation, Hebrew University of Jerusalem, Israel.

Hamdy, R. and Dorgham, M. (2018). Intermittent study of benthic fauna in the Eastern Harbour of Alexandria, Egypt. Egypt. J. Aquat Biol. & Fish., 22(4): 209-223. https://bit.ly/3hXjzHm

Hamed, M. A. (2003). Hydrochemistry and nutrients of Lake Manzala, Egypt. J. Egypt. Acad. Soc. Environ. Develop. (Environmental Studies), 2 (P): 29-48.

Hamza, A.; Enajjar, S.; Karaa, S. and Bradai M. N. (2018). Record of the invasive red sea mussel *Brachidontes pharaonis* (BIVALVIA: MYTILIDAE) from the lagoon of boughrara (southern Tunisia, central mediterranean sea). Institut National des Sciences et Technologies de la Mer (Centre de Sfax) BP. 1035 – 3018 Sfax. https://bit.ly/3hTV0eg

Hussein, R.; El-Aziz, A.; Arafa, A. and El-Sebaie, O. (2013). Impact of Alexandria Corniche Road Widening on Mediterranean Sea Water Quality, Egypt. J. High Inst. of Pub. Heal., 43(2): 175-184. https://bit.ly/3k4K9kg

Iskander, M. M. (2017). Impact of the construction phase on the coastal structure behavior. 4th International Conference on Environmental Studies and Research"Smart Sustainable Environment" Sharm El Sheikh: 27-29.

Iskander, M. M.; Frihy, O. E.; El Ansary, A. E.; Abd El Mooty, M. M. and Nagy, H. M. (2007). Beach impacts of shore-parallel breakwaters backing offshore submerged ridges, Western Mediterranean Coast of Egypt. J. Enviro. Manag., 85(4): 1109-1119. https://bit.ly/3yM1Itt

Khalil, M.T.; Shakir, S.H.; Saad, A.A.; El Shabrawy, G.M. and Hassan, M.M. (2008). Physico-chemical environment of lake Edku, Egypt. Egyptian Journal of Aquatic Biology and Fisheries, 12(2), 119-132.

Khalil, M.T.; Saad, A.A.; Fishar, M.R. and Bedir, T.Z. (2013). Ecological studies on macrobenthic invertebrates of Bardawil wetland, Egypt. World Environment, 3(1), 1-8. https://bit.ly/36Caqih

Khalil, M.T.; Saad, A.A.; Ahmed, M.H.; El Kafrawy, S.B. and Emam, W.W. (2016). Integrated field study, remote sensing and GIS approach for assessing and monitoring some chemical water quality parameters in Bardawil lagoon, Egypt. Int J Innov Res Sci, Eng Technol, 5(8), 10-15680. https://bit.ly/3hsnNYm

Masria, A.; Nadaoka, K.; Negm, A. and Iskander, M. (2015). Detection of shoreline and land cover changes around Rosetta promontory, Egypt, based on remote sensing analysis. Land, 4(1): 216-230. https://bit.ly/36pcg5O

Mifsud, C. and Cilia, D. P. (2009). On the presence of a colony of *Brachidontes pharaonis* (P. Fischer, 1870) (Bivalvia: Mytilidae) in Maltese waters (Central Mediterranean). Triton, 20, 20-22. https://bit.ly/3ADJxIx

Ming, D. and Chiew, Y.M. (2000). Shoreline changes behind a detached breakwater. Journal of Waterway, Port, Coastal, and Ocean Engineering, 126(2): 63-70. https://bit.ly/3xxteuI

Moran, P.J. and Grant, T.R. (1991). Transference of marine fouling communities between polluted and unpolluted sites: impact on structure. Enviro. Poll., 72(2): 89-102. https://bit.ly/2Vc8biX

Oliver, P. G. (1992). The Bivalve Seashells of the Red Sea. An Identification Guide. Christa Hemmen Verlag andThe National Museum of Wales, p. 330, 46 cols. pls.

Radwan, N. A. (2014): Biological and molecular studies on selected molluscs collected from the Egyptian coastal water. Ph. D. Thesis, Faculty of Science, Suez Canal University, Egypt.194pp.

Razek, F. A. A.; El-Deeb, R. S.; Abdul-Aziz, K. K.; Omar, H. A. and Khafage, A. R. (2017). Hermaphroditism in *Brachidontes pharaonis* (Fischer, 1876) (Bivalvia: Mytilidae) from the Alexandria Coast, Egypt. Egypt. J. Aquat. Res, *43*(3), 265-268. https://bit.ly/2TJQNlw

Safriel, U.N.; Gilboa, A. and Felsenburg, T. (1980). Distribution of rocky intertidal mussels in the Red Sea coasts of Sinai, the Suez Canal, and the Mediterranean coast of Israel, with special reference to recent colonizers. J. of Biogeo., 39-62. https://bit.ly/3wCAsMU

Sarà, G.; Vizzini, S. and Mazzola, A. (2003). Sources of carbon and dietary habits of new Lessepsian entry *Brachidontes pharaonis* (Bivalvia, Mytilidae) in the western Mediterranean. Marine Biology, 143(4), 713-722. https://bit.ly/3yFJiuw

Sarà, G.; Romano, C.; Widdows, J. and Staff, F. J. (2008). Effect of salinity and temperature on feeding physiology and scope for growth of an invasive species (*Brachidontes pharaonis*-Mollusca: Bivalvia) within the Mediterranean Sea. J. Exper. Mar. Biol. and Eco., 363(1-2): 130-136. https://bit.ly/3hpNqsI

Soliman, A.; Elsharnouby, B. and Elkamhawy, H. (2014). Shoreline Changes Due to Construction of Alexandria Submerged Breakwater, Egypt. In ICHE 2014. Proceedings of the 11th International Conference on Hydroscience and Engineering (pp. 675-684) ISBN 978-3-939230-32-8. https://bit.ly/3AM94PQ

Sousa, J. A.; Magariños, B.; Eiras, J. C.; Toranzo, A. E. and Romalde, J. L. (2001). Molecular characterization of Portuguese strains of Yersinia ruckeri isolated from fish culture systems. J. Fish Dise., 24(3): 151-159. https://bit.ly/3AKbfmU

Therriault, T. W. and Kolasa, J. (2000). Explicit links among physical stress, habitat heterogeneity and biodiversity. Oikos, 89(2): 387-391. https://bit.ly/3jZAjjM

Warburg, M. R.; Davidson, D.; Yifrach, H.; Sayag, L. and Tichomirova, Y. (2012). Changes in population structure and body dimensions of two xanthid crabs: A long-term study in a single boulder-shore. Arthropods, 1(2): 40. https://bit.ly/3wsthGL

Zenetos, A.; Çinar, M. E.; Pascucci-Papadopoulou M. A.; Harmelin, J. G.; Furnari, G.; Andaloro, F. and Zibrowius, H. (2005). Annotated list of marine alien species in the Mediterranean with records of the worst invasive species. Medi. mar. sci., 6(2): 63-118. https://bit.ly/3wuvMbH

Zgozi, S. W.; Haddoud, D. A. and Rough, A. (2002). Influence of environmental factors on distribution and abundance of macrobenthic organisms at Al Gazala lagoon (Libya). Technical Report of Marine Research Center of Tajura, pp.23-27.

Zisserman, J.A. and Johnson, H.K. (2002). Modeling morphological processes in the vicinity of shore-parallel breakwaters. Coastal Engineering, 45(3-4): 261-284. https://bit.ly/3k1rHZU